LAND-COVER MONITORING USING TIME-SERIES HYPERSPECTRAL DATA VIA FRACTIONAL-ORDER DARWINIAN PARTICLE SWARM OPTIMIZATION SEGMENTATION

Naoto Yokoya[1,2,3] and Pedram Ghamisi[1,2]

[1]Remote Sensing Technology Institute (IMF), German Aerospace Center (DLR), Germany
[2]Signal Processing in Earth Observation (SiPEO), Technische Universität München (TUM), Germany
[3]Department of Advanced Interdisciplinary Studies, University of Tokyo, Japan

ABSTRACT

This paper presents a new method for unsupervised detection of multiple changes using time-serires hyperspectral data. The proposed method is based on fractional-order Darwinian particle swarm optimization (FODPSO) segmentation. The proposed method is applied to monitor land-cover changes following the Fukushima Daiichi nuclear disaster using multitemporal Hyperion images. Experimental results indicate that the integration of segmentation and a time-series of hyperspectral images has great potential for unsupervised detection of multiple changes.

***Index Terms*—** FODPSO-based segmentation, unsupervised change detection, multiple changes, land-cover monitoring, time-series analysis.

1. INTRODUCTION

Unsupervised change detection using multitemporal hyperspectral data has received great attention in the last decade since ground reference is not available in many practical cases of change detection. In particular, the detection of multiple changes is of great interest to utilize rich spectral information in hyperspectral data. One of the major approaches is based on linear transformation, such as canonical correlation analysis (CCA) [1] and principal component analysis (PCA) [2]. Multivariate alteration detection (MAD) analyzes differences between CCA variates and it has been successfully investigated in a wide range of applications using multitemporal spectral images. Change vector analysis was also commonly considered in various applications using multispectral images [3] and it has been extended to detection of multiple changes for multitemporal hyperspectral images [4].

Image segmentation has been extensively studied owing to its meaningful image representation, which enables object-based analysis. Segmentation has been applied to change detection using high-resolution remote sensing images in [5]. However, to the best of the authors' knowledge, very few publications are available in the literature in which segmentation is applied for unsupervised detection of multiple changes using time-series hyperspectral data.

Among different segmentation approaches, thresholding-based techniques have gained attention in computer vision and remote sensing [6]. One common way to select optimal thresholds is the exhaustive Otsu criterion [7]. However, this approach is computationally expensive since for finding $n-1$ optimal thresholds, it demands to evaluate its corresponding fitness $n(L-n+1)^{n-1}$ times [8]. For the sake of simplicity, the task of determining $n-1$ optimal thresholds for n-level image thresholding can be formulated as a multidimensional optimization problem. Recently, an extension of particle swarm optimization (PSO) was proposed, which considers two modifications: (1) fractional calculus to control the convergence rate of the algorithm [9, 6], and (2) multiple swarms of test solutions in which each swarm moves just like an ordinary PSO with a few punishment and reward rules. The FODPSO was successfully compared with PSO families for some benchmark mathematical tests in [9] and for thresholding-based segmentation in [6].

In this paper, we present a new method for unsupervised detection of multiple changes based on FODPSO-based segmentation using a set of time-series hyperspectral data. The proposed method is applied for the detection of land-cover changes following the Fukushima Daiichi nuclear disaster using four temporal Hyperion images. The contributions of this work are twofold: 1) FODPSO-based segmentation is applied for change detection for the first time in the remote sensing community; and 2) the potential of combining segmentation and a time-series of hyperspectral images for land-cover monitoring is validated via a case study.

The rest of the paper is organized as follows: Section 2 describes materials used in this study. Section 3 is devoted to methodology. Section 4 presents experimental results. Section 5 wraps up the paper by providing the main concluding remarks.

This research has been partly supported by Alexander von Humboldt Fellowship for postdoctoral researchers.

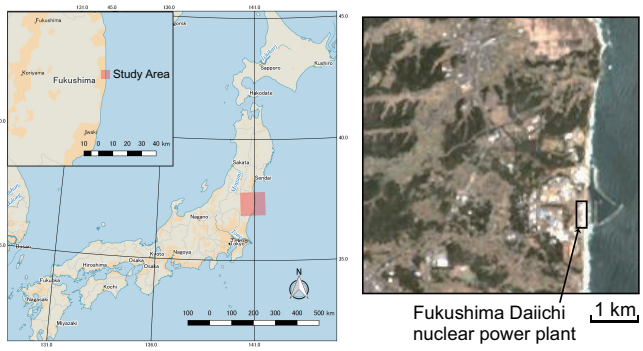

Fig. 1: (Left) Location of the study area and (right) color composite of Hyperion data taken on April 29, 2012.

2. MATERIALS

2.1. Study Area

The study area is on the Fukushima Daiichi Nuclear Power Plant ($37°25'16''$, $141°1'58''$), Fukushima, Japan, and its adjacent areas (Fig. 1). The Great East Japan Earthquake and the tsunami damaged the power plant, resulting in meltdowns and the leakage of radioactive materials. Since the disaster, visiting on site is forbidden and storage tanks have been built to store polluted water. Many of the abandoned areas have been covered by weeds.

2.2. Data and Preprocessing

The data set is composed of four temporal Hyperion images acquired over the study area on April 29, 2012, May 6, 2013, May 25, 2014, and May 2, 2015 [10]. All the images were first co-registered using geocoordinate information and further registered using phase-correlation-based image matching if a misregistration of more than one pixel is detected. Image registration was performed only by shifting the whole image at a pixel scale to avoid interpolation while keeping the same spatial resolution. We used 156 bands (bands 8–57, 79–117, 135–165, 183–185, 188–220) after removing bands that either include only zero values or influenced by strong water vapor absorption. ATCOR was used for atmospheric correction [11]. Atmospheric normalization (relative process) was further performed to mitigate residuals of non-optimal atmospheric correction. We adopted a pseudo-invariant-feature-based method, which corrects images using pixels whose spectral reflectance is consistent over time. Color composite images of the data set after atmospheric normalization are shown in the first row of Fig. 3.

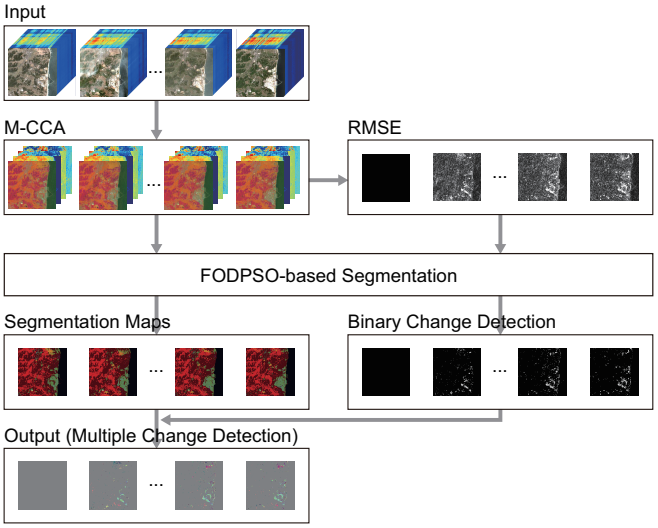

Fig. 2: Flowchart of the proposed method.

3. METHODOLOGY

3.1. Change Detection via Segmentation

The proposed method consists of three parts: 1) dimensionality reduction; 2) segmentation; and 3) multiple change detection. Fig. 2 shows the flowchart of the proposed methodology, which can be briefly explained as follows.

1. First multiset canonical correlation analysis (M-CCA) [12] is performed on a set of time-series hyperspectral data. Lower-order canonical variates, which represent more than 99% of the variance contained in the input data, are used for further processing assuming that they can explain major variations of the surface. Root mean square errors (RMSEs) between a master image (e.g., the first temporal image) and the others are calculated using these canonical variables to obtain the degree of changes.

2. FODPSO-based segmentation is performed on both a set of M-CCA images and that of RMSE maps to obtain segmentation maps and binary change detection maps, respectively. M-CCA images of each order or RMSE maps are spatially stacked before performing segmentation. The level of segmentation for the M-CCA images can be defined by taking into account prior knowledge about an approximate number of land-cover classes in the study area. The level of segmentation for the RMSE maps is set to two to conduct binary change detection.

3. Multiple changes with various degrees of changes are detected by generating the difference of segmentation between the master image and the others. They are integrated with the binary change detection maps and fi-

nally multiple change detection maps are obtained as the output.

More details of FODPSO-based segmentation, which forms the basis for the proposed method, are provided in the following section.

3.2. FODPSO-based Segmentation

As suggested in [6], the simplest and computationally most efficient fitness function to define optimal thresholds in thresholding-based segmentation approaches is the one that maximizes the between-class variance. In order to find optimal thresholds t_j^{Co}, the following fitness function can be formulated:

$$\varphi^{Co} = \max_{1 < t_1^{Co} < \ldots < t_{n-1}^{Co} < L_{Co=\{R,G,B\}}} \sigma^2_{B^{Co}}(t_j^{Co}) \quad (1)$$

where L is the intensity level in each *RGB* component of the input image. These levels are in the range $\{0, 1, 2, \ldots, L\text{-}1\}$. For example, the number of intensity levels L for an 8-bit image is between 0 and 255. Co represents the component of the image. Here, we discuss the the approach for an RGB image but it can be simply generalized to high dimensional data.

FODPSO was proposed in [6] for image segmentation to address the main shortcoming of a simple PSO (i.e., the stagnation of particles around sub-optimal solutions). In more detail, the following modifications have been taken into account:

1. FODPSO is composed of many simultaneous parallel PSO on the same test problem and considers a simple natural selection mechanism. When a search tends to a sub-optimal solution, the search in that area is simply discarded and another area is searched instead. For more information regarding how these rewards and punishments can be applied, please see [6, 8, 13].

2. Fractional calculus is used to control the convergence rate of the algorithm. This method has been further investigated for gray scale and hyperspectral image segmentation and feature selection in [6, 14] and [15], respectively. The main advantage of fractional calculus is that while an integer-order derivative just implies a finite series, the fractional-order derivative requires an infinite number of terms. Therefore, integer derivatives are considered as "local" operators, while fractional derivatives have, implicitly, a "memory" of all past events, which is useful to control the dynamic of each swarm.

In order to mathematically derive the FODPSO, in each step t, the fitness value (i.e., Eq. (1)) is estimated. To model the swarm, each particle *n* flies in a multidimensional search space considering the position ($\mathbf{x}_n[t]$), and velocity ($v_n[t]$), which are highly dependent on local best ($\breve{x}_n[t]$) and global best ($\breve{g}_n[t]$) information as follows:

$$v_n^s[t+1] = \quad (2)$$
$$w_n^s[t+1] + \rho_1 r_1(\breve{g}_n^s[t] - \mathbf{x}_n^s[t]) + \rho_2 r_2(\breve{x}_n^s[t] - \mathbf{x}_n^s[t]),$$

$$w_n^s[t+1] = \quad (3)$$
$$\alpha v_n^s[t] + \frac{1}{2}\alpha(1-\alpha)v_n^s[t-1] + \frac{1}{6}\alpha(1-\alpha)(2-\alpha)v_n^s[t-2]$$
$$+ \frac{1}{24}\alpha(1-\alpha)(2-\alpha)(3-\alpha)v_n^s[t-3].$$

The superscript '*s*' shows the number of each swarm. The coefficients ρ_1 and ρ_2 control the inertial influence of the global best and the local best, respectively. In general, ρ_1 and ρ_2 are constant integer values, which represent "cognitive" and "social" behavior of each particle with $\rho_1 + \rho_2 < 2$ [16]. The parameters r_1 and r_2 are random vectors in which each unit generally is a uniform random number between 0 and 1. These random vectors are considered to increase the randomness behavior of each particle to increase the diversity of the swarm in order to avoid getting trapped in local optimum. The fractional coefficient α can be considered as a weight to control the influence of past events for determining a new velocity, $0 < \alpha < 1$ [6]. A small α causes the particles ignore their previous activities. In this way, the system dynamics will be ignored and become susceptible to get stuck in a local solution (i.e., exploitation behavior). In contrast, a large value of α forces the particles to have a more diversified behavior, which allows exploration of new solutions and improves the long-term performance (i.e., exploration behavior). However, if the exploration level is too high, then the algorithm may take longer to find the global solution. Based on [16], a good α value can be traced in the range of 0.6 to 0.8. In this work, this value is set to 0.65.

4. EXPERIMENTAL RESULTS

Fig. 3 shows the experimental results obtained by our method using the four Hyperion images. Color composites of reflectance data, M-CCA variates, FODPSO-based segmentation, and final change detection maps are shown in rows from top to bottom of Fig. 3(a). M-CCA images are correlated each other compared to those of reflectance data as shown in the second row of Fig. 3(a). This implies that M-CCA successfully extracts surface features as the low-order canonical variates by exploring common spatial patterns included in all the multitemporal images. Residual signals that appear in a specific temporal image due to various atmospheric conditions can be excluded from the low-order canonical variates, which can be seen from the images taken on May 6, 2013. Consistent segmentation results were obtained among the multitemporal images by performing thresholding-based

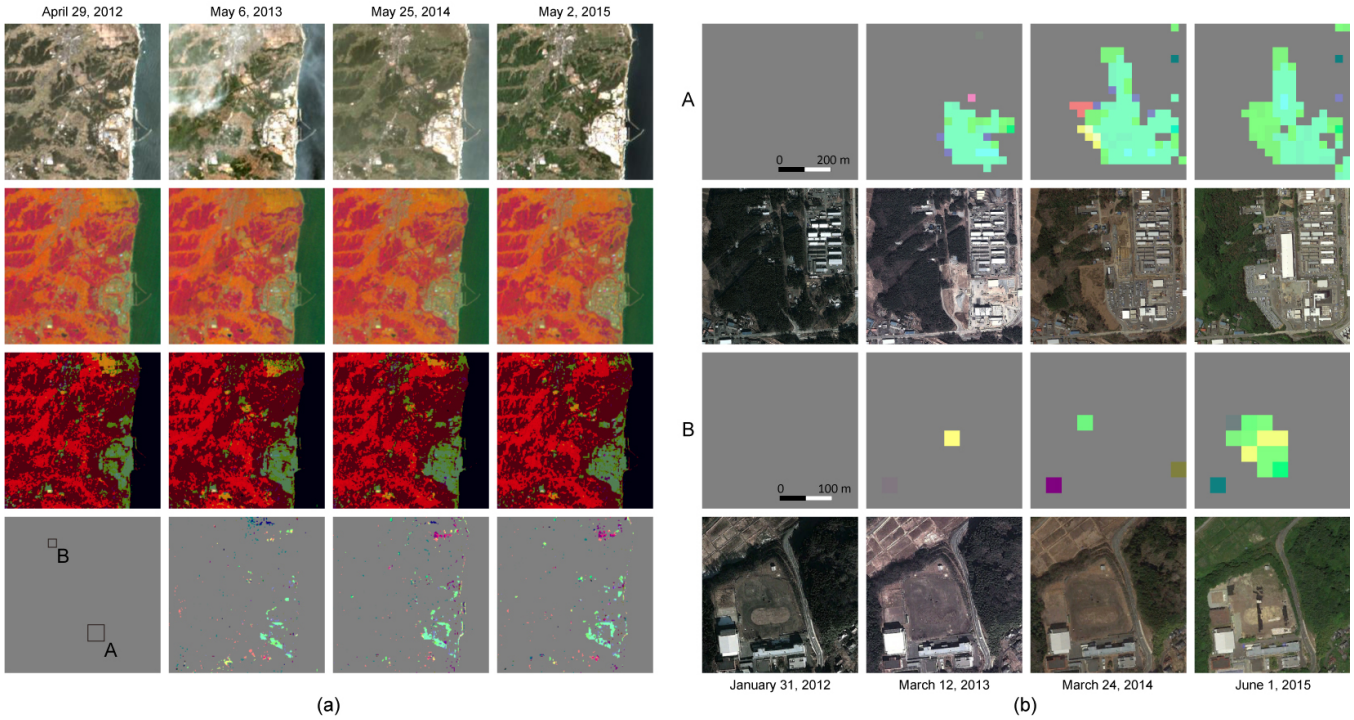

Fig. 3: (a) Color composites of reflectance data, M-CCA, FODPSO segmentation, and detected changes from top to bottom rows obtained from four temporal Hyperion data. (b) Enlarged images of change detection maps at areas A and B in (a) and corresponding high-resolution images from Google Earth (Google, DigitalGlobe).

segmentation to the spatially stacked M-CCA images. Owing to this property, it is easy to discriminate multiple changes by subtracting segmentation results.

In the fourth row of Fig. 3(a), multiple changes are clearly shown in different colors. For example, light green pixels around the power plant indicate changes from vegetation to man-made objects, and hot pink pixels in the Northeast correspond to changes from soil to vegetation due to the increase of weeds. Fig. 3(b) shows the enlarged images of change detection maps at areas A and B in Fig. 3(a) and their corresponding high-resolution images obtained from Google Earth (Google, DigitalGlobe). These high-resolution images were taken on January 31, 2012, March 12, 2013, March 24, 2014, and June 1, 2015, which are the closest acquisition dates with those of the Hyperion images. In the area A, it can be seen that deforestation and construction of man-made objects are clearly detected by the proposed method. The area B includes a schoolyard, where bags filled with radioactive waste from decontamination efforts were started to be temporarily stored in 2015. This change is also detected by the proposed method.

5. CONCLUSION

In this paper, we presented a new method for unsupervised detection of multiple changes for land-cover monitoring using time-series hyperspectral data. In this paper, FODPSO-based segmentation was proposed to use for unsupervised change detection. The potential of our method was validated via a case study that analyzes land-cover changes following the Fukushima Daiichi nuclear disaster using four temporal Hyperion images. Experimental results showed that the presented method is capable of detecting multiple changes, such as deforestation, construction of man-made objects, and increasing weeds in the considered study area. Our future research includes numerical validation and an extension of the method to handle multisensor time-series data.

6. REFERENCES

[1] M. Frank and M. Canty, "Unsupervised change detection for hyperspectral images," in *Proc. 12th JPL Airborne Earth Sci. Workshop*, 2003.

[2] V. Ortiz-Rivera, M. Vélez-Reyes, and B. Roysam, "Change detection in hyperspectral imagery using temporal principal components," in *Algorithms Technologies for Multispectral, Hyperspectral, and Ultraspectral Imagery XII*, 2006, vol. 6233.

[3] W. A. Malila, "Change vector analysis: An approach for detecting forest changes with landsat," in *6th Annu. Symp. Mach. Process. Remotely Sensed Data*, 1980.

[4] S. Liu, L. Bruzzone, F. Bovolo, M. Zanetti, and P. Du, "Sequential spectral change vector analysis for iteratively discovering and detecting multiple changes in hyperspectral images," *IEEE Trans. Geosci. Remote Sens.*, vol. 53, no. 8, pp. 4363–4378, August 2015.

[5] L. Wu, Z. Zhang, Y. Wang, and Q. Liu, "A segmentation based change detection method for high resolution remote sensing image," *Pattern Recognition*, vol. 483, pp. 314–324, 2014.

[6] P. Ghamisi, M. S. Couceiro, J. A. Benediktsson, and N. M. F. Ferreira, "An efficient method for segmentation of images based on fractional calculus and natural selection," *Expert Syst. Appl.*, vol. 39, no. 16, pp. 12407–12417, 2012.

[7] N. Otsu, "A threshold selection method from gray-level histogram," *IEEE Trans. Syst. Man Cyber.*, vol. 9, pp. 62–66, 1979.

[8] M. S. Couceiro and P. Ghamisi, *Fractional Order Darwinian Particle Swarm Optimization: Applications and Evaluation of an Evolutionary Algorithm*, Springer, Londen, 2015.

[9] M. S. Couceiro, R. P. Rocha, N. M. F. Ferreira, and J. A. T. Machado, "Introducing the fractional order Darwinian PSO," *Sig., Image and Vid. Process.*, vol. 102, no. 1, pp. 8–16, 2007.

[10] N. Yokoya and X. X. Zhu, "Graph regularized coupled spectral unmixing for change detection," in *7th WHISPERS*, 2015.

[11] R. Richter and D. Schläpfer, *Atmospheric/Topographic Correction for Satellite Imagery: Atcor 2/3 Users Guide*, 2015.

[12] J. R. Kettenring, "Canonical analysis of several sets of variables," *Biometrika*, vol. 58, pp. 433 – 451, 1971.

[13] J. A. Benediktsson and P. Ghamisi, *Spectral-Spatial Classification of Hyperspectral Remote Sensing Images*, Artech House Publishers, INC, Boston, USA, 2015.

[14] P. Ghamisi, M. S. Couceiro, F. M.L. Martins, and J. A. Benediktsson, "Multilevel image segmentation approach for remote sensing images based on fractional–order Darwinian particle swarm optimization," *IEEE Trans. Geos. Remote Sens.*, vol. 52, no. 5, pp. 2382–2394, 2014.

[15] P. Ghamisi, M. S. Couceiro, and J. A. Benediktsson, "A novel feature selection approach based on FODPSO and SVM," *IEEE Trans. Geos. Remote Sens.*, vol. 53, no. 5, pp. 2935–2947, 2015.

[16] M. S. Couceiro, F. M. Martins, R. P. Rocha, and N. M. Ferreira, "Mechanism and convergence analysis of a multi-robot swarm approach based on natural selection," *Jour. Intell. Rob. Sys.*, pp. 1–29, 2014.